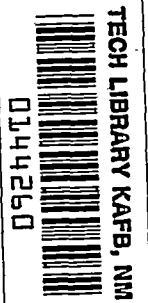


NACA RM L53H26



NACA

RESEARCH MEMORANDUM

RECENT EXPERIENCES WITH FLUTTER FAILURE
OF SWEPTBACK, TAPERED WINGS HAVING
OUTBOARD, PARTIAL-SPAN SPOILER CONTROLS

By H. Kurt Strass and Edward T. Marley

Langley Aeronautical Laboratory
Langley Field, Va.

NATIONAL ADVISORY COMMITTEE
FOR AERONAUTICS

WASHINGTON

October 5, 1953

Classification cancelled (or changed to) Unclassified
By Authority: Nase Tech Pub Announcement #108
(DO NOT CHANGE)

By.....
29 Aug 51
K

GRADE OF OFFICE

30 Mar 41
DATE



NATIONAL ADVISORY COMMITTEE FOR AERONAUTICS

RESEARCH MEMORANDUM

RECENT EXPERIENCES WITH FLUTTER FAILURE
OF SWEEPBACK, TAPERED WINGS HAVING
OUTBOARD, PARTIAL-SPAN SPOILER CONTROLS

By H. Kurt Strass and Edward T. Marley

SUMMARY

During the course of an investigation by the Langley Pilotless Aircraft Research Division regarding the effectiveness of spoilers and ailerons on sweptback tapered wings, it was necessary to test a given control configuration on wings of varying degrees of stiffness. In the process of conducting these tests, repeated wing failure was experienced with the weaker wing-spoiler configurations, whereas no failure occurred with any of the wing-aileron models. An investigation which was conducted by means of rocket-propelled test vehicles in free flight showed that the cause of the repeated failures was flutter of the bending-torsion type.

INTRODUCTION

During the course of an investigation by the Langley Pilotless Aircraft Research Division regarding the effectiveness of spoiler-type controls (ref. 1) on sweptback wings of varying degrees of stiffness, wing failure was encountered repeatedly on the models having the more flexible wings.

As part of an effort to determine the cause of the failure of these particular wings, additional tests were made using specially instrumented low-acceleration rocket-propelled test vehicles. The results of these tests are not conclusive because of the lack of extensive data, but the data presented herein should be of interest to aircraft and missile designers who contemplate using spoiler-type wing controls in the transonic and supersonic speed ranges.

SYMBOLS

a	distance in wing semichords from midchord to elastic-axis position, positive rearward, $2x_0 - 1$
b	semichord of wing measured perpendicular to elastic axis, ft
b'	diameter of circle swept by wing tips, 3.0 ft
c	local chord measured parallel to direction of flight, in.
$c_{R/2}$	semichord at reference station, perpendicular to quarter-chord line, ft
l'	length of wing measured along elastic axis, ft
f_{h1}	wing first bending natural frequency (laboratory tests), cps
f_t	wing first torsional natural frequency (laboratory tests), cps
I_α	polar moment of inertia of wing section about elastic axis, slug-ft ² /ft
f	wing flutter frequency (measured during flight), cps
m	mass of wing per unit length along quarter-chord line, slugs/ft
m_c	concentrated couple, applied near wing tip in plane parallel to free stream and normal to wing-chord plane, ft-lb
r_α	nondimensional radius of gyration of wing section about elastic axis, $(I_\alpha/mb^2)^{1/2}$
x_0	distance of elastic axis of wing section behind leading edge, fraction of chord
x_α	distance in semichords from wing elastic axis to wing center-of-gravity position
$(\theta/m_c)_r$	wing torsional-flexibility parameter measured at midpoint of control span in plane parallel to free stream and normal to wing-chord plane, radians/ft-lb
A	aspect ratio, b'^2/S

A_g	geometric aspect ratio of one wing panel, $\frac{\text{Exposed semispan}}{\text{Mean streamwise chord}}$
E	Young's modulus of elasticity, lb/sq in.
G	shear modulus of elasticity, lb/sq in.
I	moment of inertia of streamwise airfoil cross section about chord plane, in. ⁴
J	torsional stiffness constant of streamwise airfoil cross section in plane parallel to direction of flight, in. ⁴
$(EI)_e$	effective flexural stiffness parameter of streamwise airfoil cross section, lb-in. ²
$(GJ)_e$	effective torsional stiffness parameter of streamwise airfoil cross section, lb-in. ²
M	Mach number
V	flight-path velocity, fps
S	area of two wings measured to model center line, 2.24 square feet
θ	angle of twist produced by m at any section along span in plane parallel to free stream and normal to wing-chord plane, radians
κ	wing mass-density ratio at flutter, $\pi \rho b^2/m$
λ	taper ratio, ratio of tip chord to chord at model center line
Λ	angle of sweepback of quarter-chord line, deg
ρ	density of air, slugs/cu ft

Subscripts:

1	first evidence of flutter
2	wing failure
R	calculated value based on two-dimensional flow

MODELS AND INSTRUMENTATION

Models

The models used in these tests consisted of two types and are shown in figures 1 and 2. The first type shown in the photograph of figure 1(a) and sketch of figure 2(a) was flown as part of a control-effectiveness investigation and is fully described in references 1 and 2. The second type, of which two models were flown, is described in the photograph and sketch of figures 1(b) and 2(b). This type was essentially a 5-inch cordite rocket motor to which an instrumented nose section was added and three wing panels were spaced 120° apart around the fuselage.

Wings.- The wings on all models were swept back 45° at the quarter-chord line and had an aspect ratio of 4.0, taper ratio 0.6, and NACA 65A006 airfoil sections parallel to the free stream. These wings had either spoiler- or flap-type fixed controls and the wing construction varied with the particular model. The addition of a spoiler or a deflected aileron caused no appreciable change in the structural characteristics. The geometric characteristics of the wing-control configuration used on each model are presented in figure 3. Figure 4 presents closeup photographs of the spoiler controls that were tested. For reference, figure 5 presents the variation of the effective flexural and torsional parameters with extent of exposed span for wing construction a (see fig. 3(d)).

Instrumentation

A spinsonde transmitter which is incapable of detecting flutter was used in determining the model rolling velocity about the flight axis (ref. 3) and was the only instrumentation used in the first type of model (fig. 1(a)). In addition to the spinsonde transmitter, the second-type model (fig. 1(b)) was equipped with a two-channel telemeter designed to transmit the wing bending and torsion frequencies detected by strain gages located near the root on one wing of each model. The type of instrumentation used on each model is listed in table I.

The flight tests were made at the Pilotless Aircraft Research Station, Wallops Island, Va. All models employed a two-stage rocket propulsion system capable of propelling the models to a Mach number of approximately 1.6. During flight, time histories of the flight-path velocity, rolling velocity, and wing flutter frequencies for the strain-gage equipped models, obtained by CW Doppler radar, spinsonde, and telemeter, respectively, were recorded by ground receiving stations.

RESULTS AND DISCUSSION

In order to determine the effects of aeroelasticity upon the wing-control configurations described in references 1 and 2, it was necessary to test a given control configuration on wings of varying degrees of stiffness. In the process of conducting these tests, repeated failures were experienced with the weaker wing-spoiler configurations (models 1, 2, and 3), whereas no failure occurred with any of the weaker wing-aileron configurations (model 6 is typical). No failure was experienced with any of the stiffer aileron or spoiler models (models 7 and 8 represent typical cases). Because of this fact, two specially instrumented models were constructed in order to determine the nature of the failure. The first of these special test vehicles (model 4) exhibited destructive flutter at $M \approx 1.0$. The spoilers on the second of these test vehicles (model 5) were vented by removing approximately 24 percent of the frontal area by slotting in an attempt to alleviate the severity of the flutter. However, no significantly beneficial effect of venting was observed, inasmuch as the second test vehicle also failed because of flutter at $M \approx 1.08$.

The velocity at which flutter might occur was calculated by the method of reference 4 assuming incompressible two-dimensional flow and that the mode shape of the wings during flutter could be represented in the analysis by the first bending and first torsion mode shapes of a uniform cantilever beam. The structural constants of the cantilever beam were assumed to be the same as those at the 75-percent-semispan station of the tapered wing, a procedure which has been found by past experience to give acceptable results for moderately tapered wings. The pertinent flutter parameters for models 4 and 5 are given in table II. The calculated and experimental values are presented in table III.

In reference 5, the ratio between the experimentally determined flutter speed and that calculated by the method of reference 4 was determined for a wide range of wing sweep angles, aspect ratios, and types of wing constructions. For purposes of comparison, the flight test data are presented in figure 6 in conjunction with the data from reference 5 for wings of the same plan-form shape but 4 percent thick instead of 6 percent. The data from reference 5 indicate that the basic wing would have fluttered at approximately the same velocity as that observed from the flight tests of the wing-spoiler configuration.

The significance of the apparent good agreement between the predicted and measured flutter velocities of the spoiler-equipped models is questionable at this time, because of the facts that the effect of the control is not considered in the methods of estimation and that destructive flutter did not occur on the aileron-equipped models. Nondestructive flutter may have existed during some flight phase of the wing-aileron

CONFIDENTIAL

models, but these models were not instrumented to detect flutter. Application of the simplified flutter criterion of reference 6 to models 1 to 6 indicated that flutter should have occurred.

The portions of the telemeter records showing the onset of flutter and the resulting failure of models 4 and 5 are presented in figure 7. Because the bend record for model 4 does not indicate the point where wing failure occurred with sufficient accuracy, this information was taken from a motion-picture record of the flight which indicated that all three wings came off simultaneously at approximately $M = 1.0$.

CONCLUSION

The results of this investigation show that a wing with an outboard partial-span spoiler experienced destructive flutter; whereas, a wing of the same construction but with an outboard partial-span aileron did not fail.

Langley Aeronautical Laboratory,
National Advisory Committee for Aeronautics,
Langley Field, Va., August 7, 1953.

CONFIDENTIAL

REFERENCES

1. Schult, Eugene D., and Fields, E. M.: Free-Flight Measurements of Some Effects of Spoiler Span and Projection and Wing Flexibility on Rolling Effectiveness and Drag of Plain Spoilers on a Tapered Sweptback Wing at Mach Numbers Between 0.6 and 1.6. NACA RM L52H06a, 1952.
 2. Schult, Eugene D., Strass, H. Kurt, and Fields, E. M.: Free-Flight Measurements of Some Effects of Aileron Span, Chord, and Deflection and of Wing Flexibility on the Rolling Effectiveness of Ailerons on Sweptback Wings at Mach Numbers Between 0.8 and 1.6. NACA RM L51K16, 1952.
 3. Harris, Orville R.: Determination of Rate of Roll of Pilotless Aircraft Research Models by Means of Polarized Radio Waves. NACA TN 2023, 1950.
 4. Barmby, J. G., Cunningham, H. J., and Garrick, I. E.: Study of Effects of Sweep on the Flutter of Cantilever Wings. NACA Rep. 1014, 1951. (Supersedes NACA TN 2121.)
 5. Jones, George W., Jr., and DuBose, Hugh C.: Investigation of Wing Flutter at Transonic Speeds for Six Systematically Varied Wing Plan Forms. NACA RM L53G10a, 1953.
 6. Martin, Dennis J.: Summary of Flutter Experiences As a Guide to the Preliminary Design of Lifting Surfaces on Missiles. NACA RM L51J30, 1951.
- [REDACTED]

TABLE I

TABULATED MODEL DATA

Model	Type of wing control	Instrumentation	Wing construction (see fig. 3(d))	$(\theta/m_c)_r$	Failure	Flutter
1	Spoiler, solid	Spinsonde	a	30.7×10^{-4}	Yes	Not measured
2	Spoiler, solid	Spinsonde	b	58.4	Yes	Do.
3	Spoiler, slotted	Spinsonde	b	----do----	Yes	Do.
4	Spoiler, solid	Spinsonde plus strain gages	a	30.7	Yes	Yes
5	Spoiler, slotted	Spinsonde plus strain gages	a	----do----	Yes	Yes
6	Aileron, $\delta = 9.92^\circ$	Spinsonde	a	----do----	No	Not measured
7	Spoiler	Spinsonde	Solid aluminum alloy or equivalent	4	No	Do.
8	Aileron	Spinsonde	-----do-----	----do----	No	Do.

NACA

TABLE II

PERTINENT FLUTTER PARAMETERS FOR MODELS 4 AND 5

A_g	1.78
Λ , deg	45
$c_R/2$, ft	0.238
Center-of-gravity position, percent c	46
Elastic-axis position, percent c	45
a	-0.1
$a + x_\alpha$	-0.08
r_α^2	0.2465
f_{h1} , cps	28
f_t , cps	115
b, ft	0.24
l' , ft	1.74
l/κ	115.8



CONFIDENTIAL

TABLE III

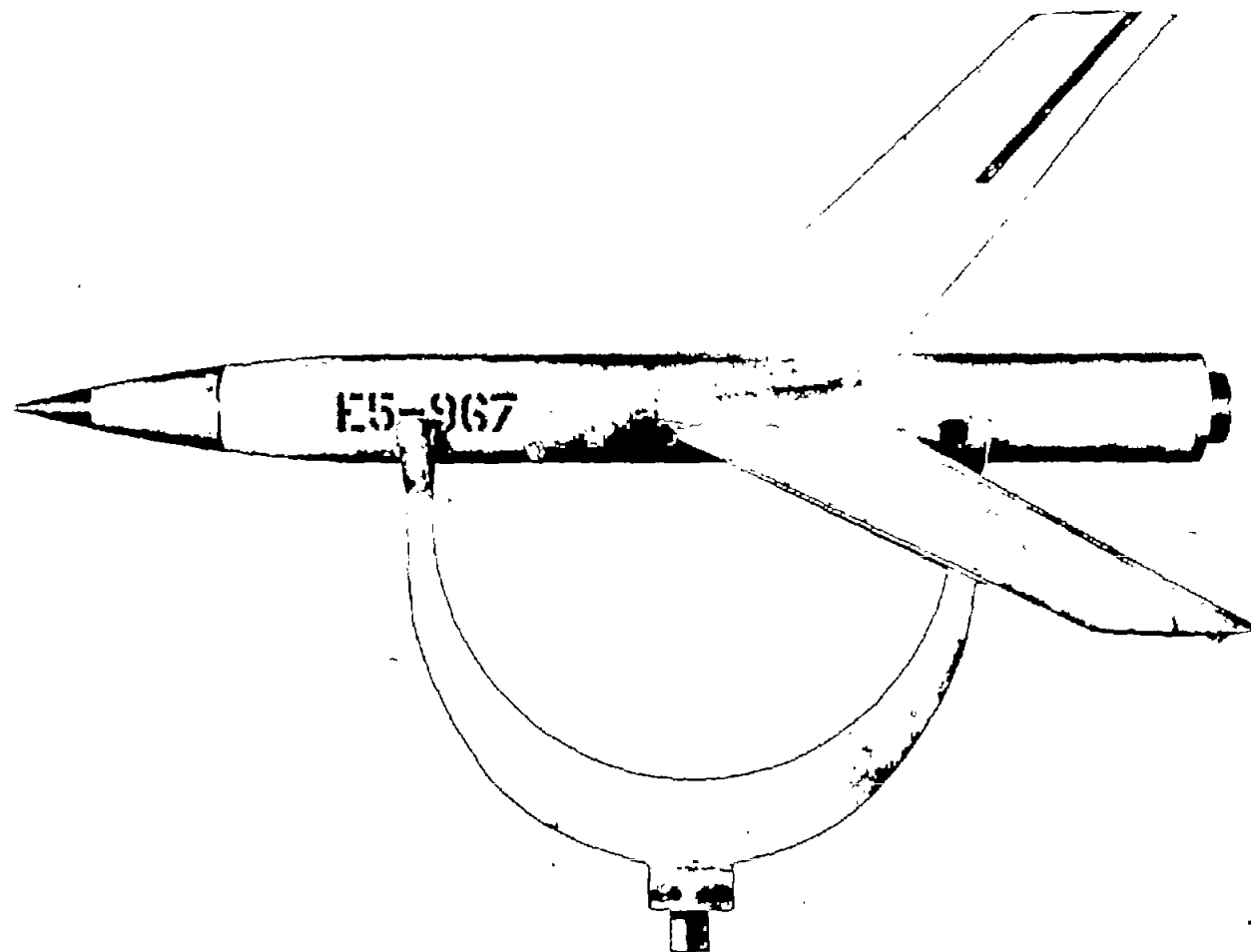
TESTS RESULTS FOR MODELS 4 AND 5

[Models 1, 2, and 3 failed in the speed range
 $800 \leq V_2 \leq 1,100$]

	Experiment		Theory (ref. 4)
	Model 4	Model 5	
M_1	0.91	0.88	
M_2	1.00	1.08	
V_1	1,042	1,025	
V_2	1,130	1,230	
V_R			983
f	54	56	51



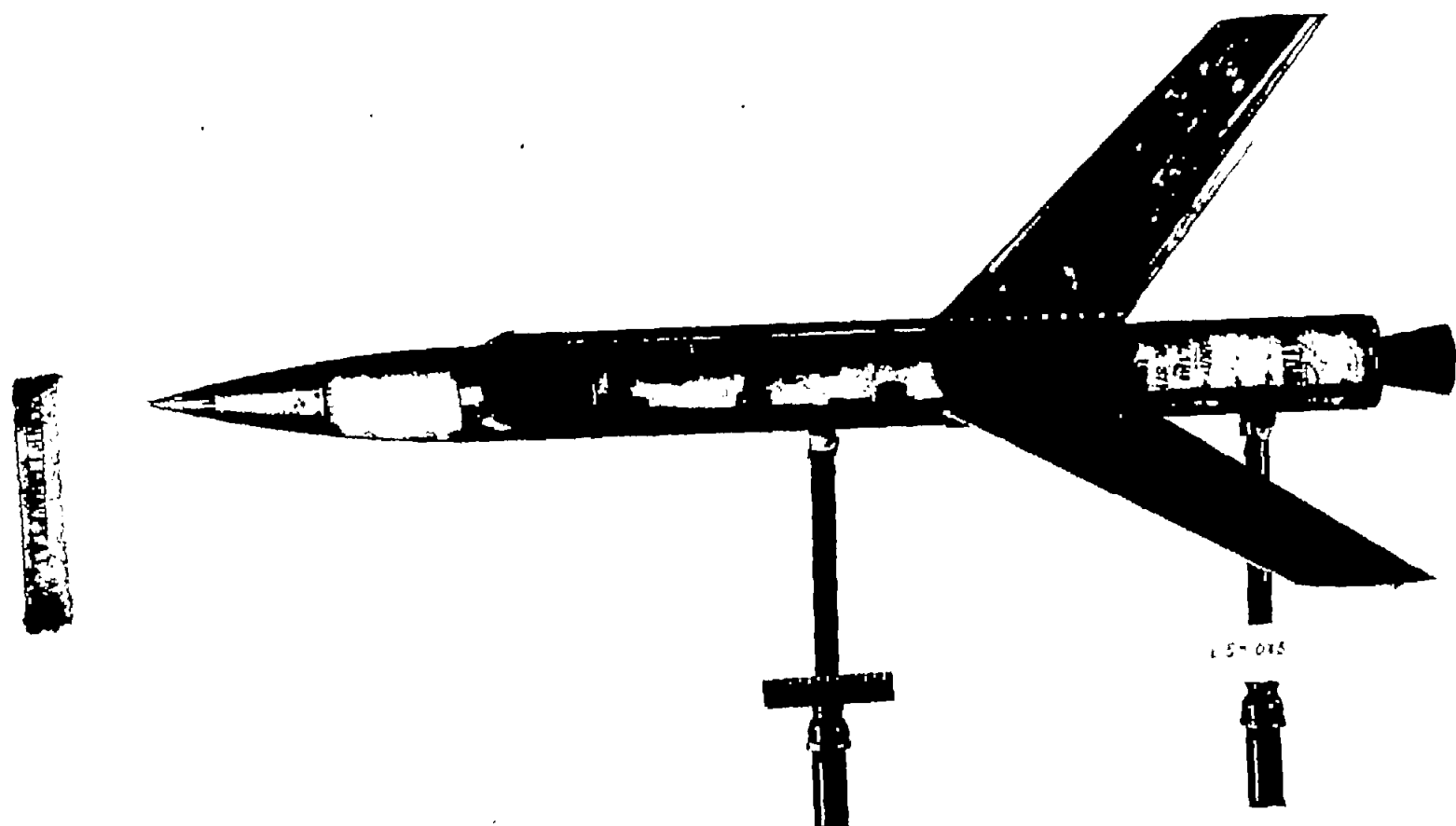
CONFIDENTIAL



(a) Models 1, 2, 3, and 6.

Figure 1.- Typical test vehicles.

L-71245



(b) Models 4 and 5.
Figure 1.- Concluded.

L-76092

NACA RM L53H26

CONFIDENTIAL

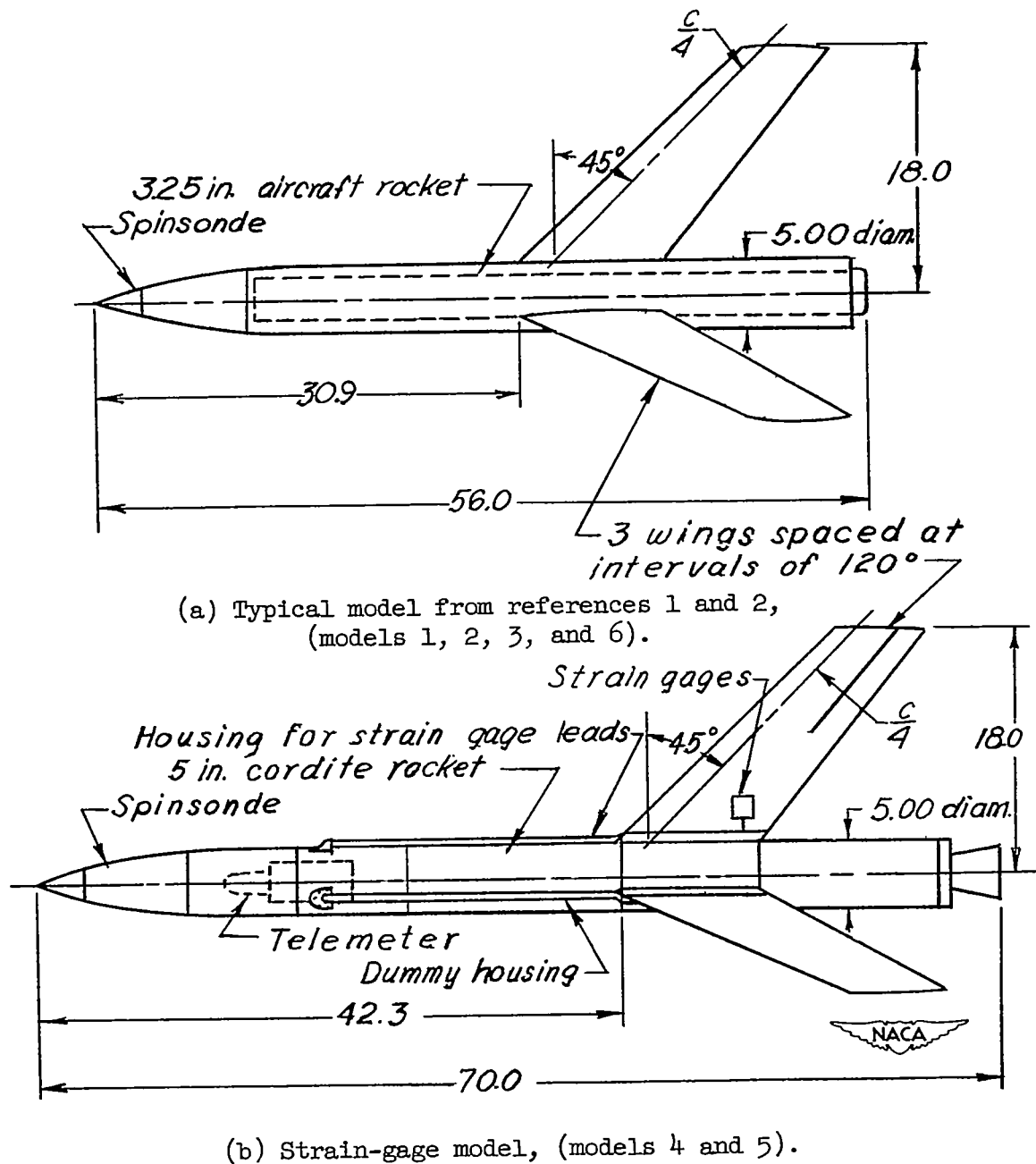
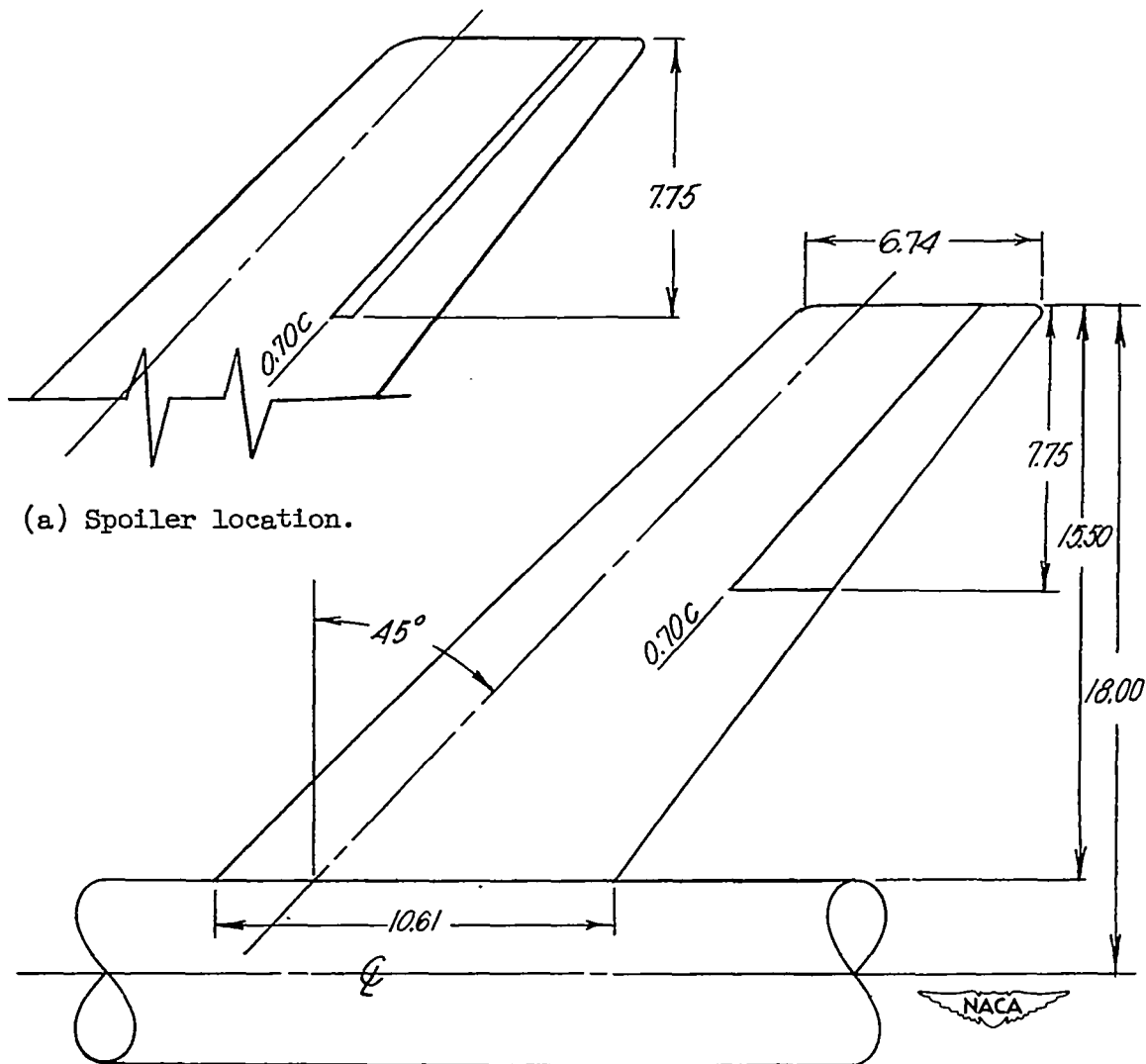
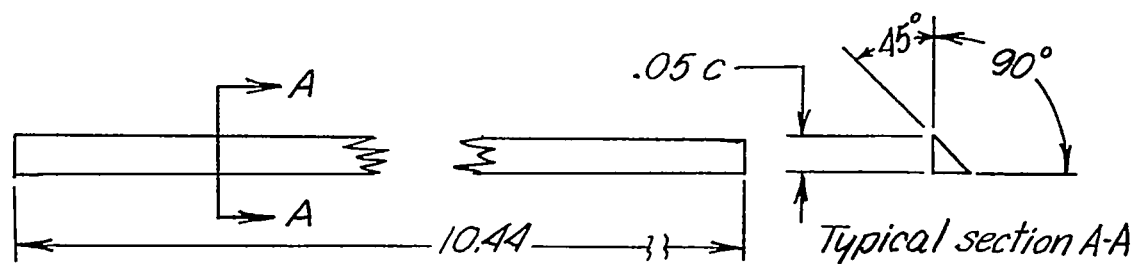
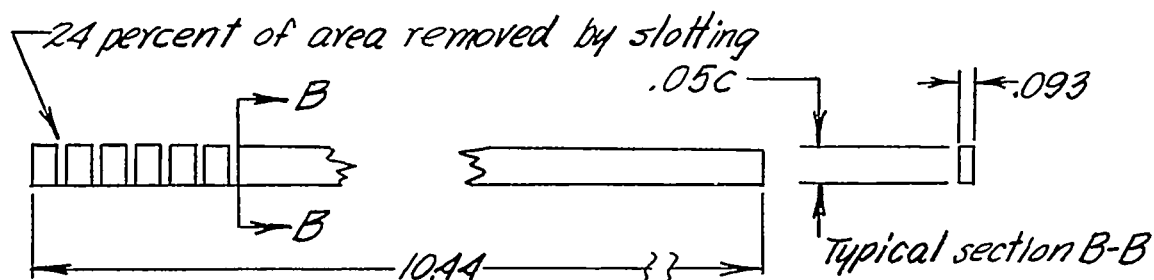


Figure 2.- General arrangement of test vehicles. All dimensions are in inches.



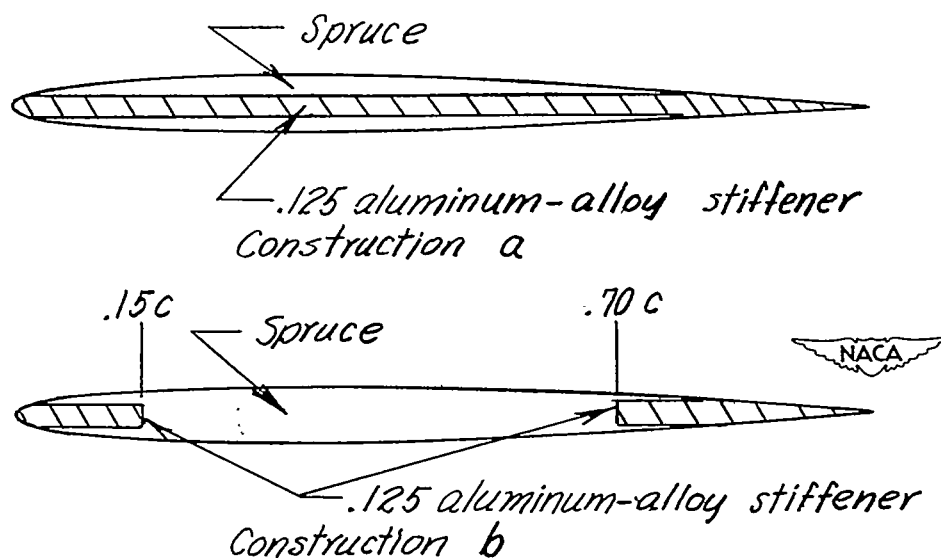
~~CONFIDENTIAL~~

Solid spoiler (models 1 to 4)



Slotted spoiler (model 5)

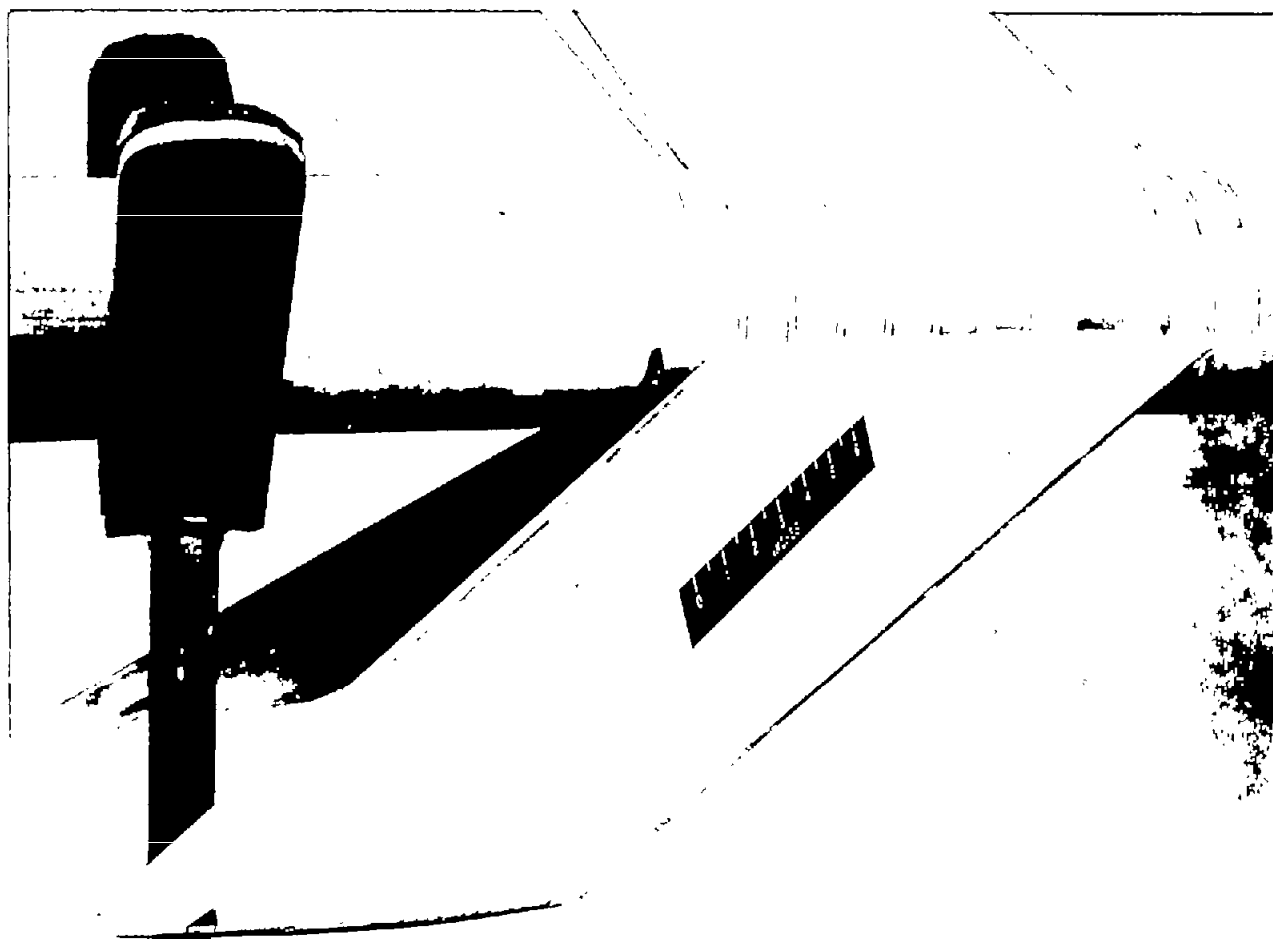
(c) Spoiler details.



(d) Typical sections.

Figure 3.- Concluded.

~~CONFIDENTIAL~~

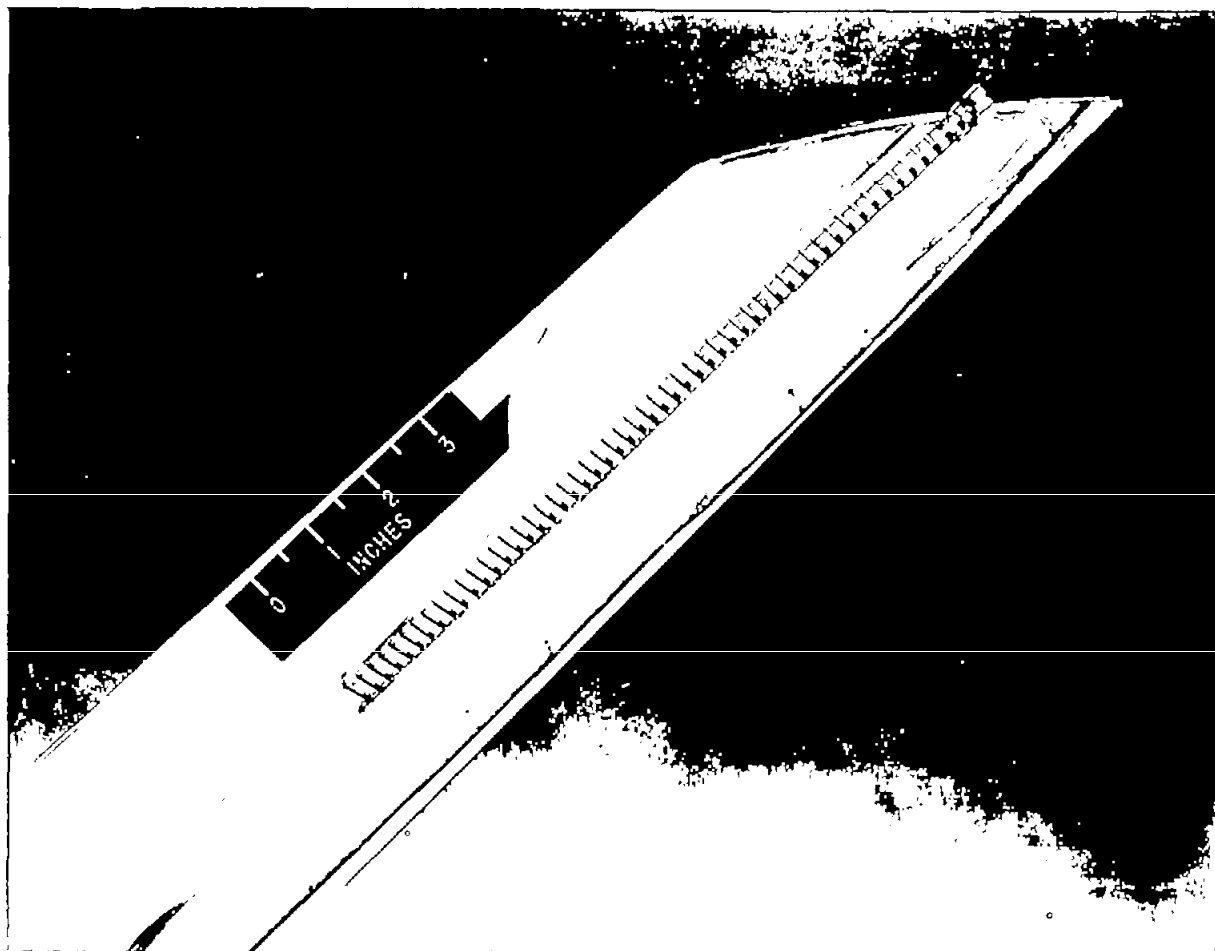


(a) Solid spoiler.

L-69044

Figure 4.- Closeup details of the spoiler controls tested.

CONFIDENTIAL



(b) Slotted spoiler.

L-70976

Figure 4.- Concluded.

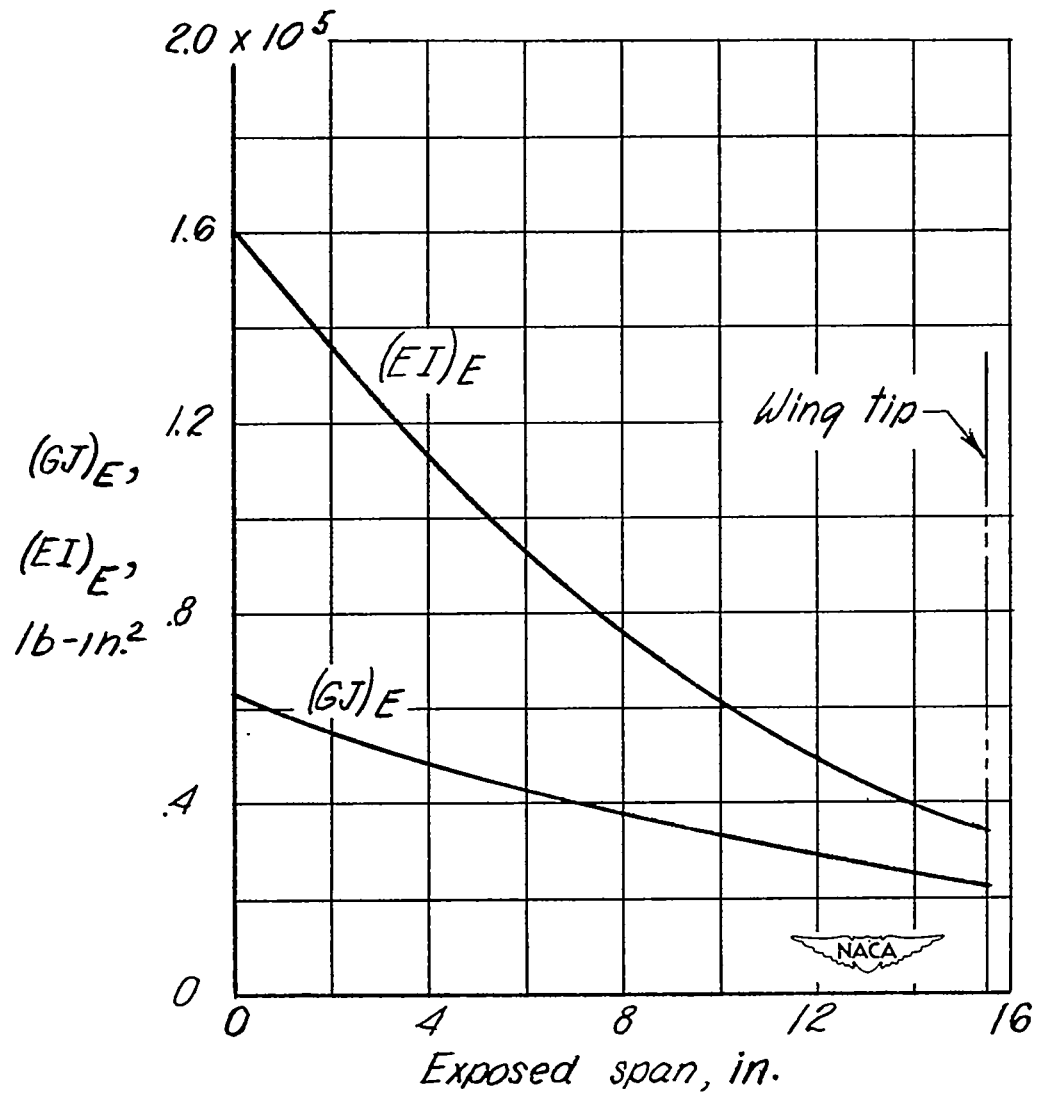


Figure 5.- Variation of effective flexural and torsional stiffness parameters with extent of exposed span for wing construction a. (see fig. 3(d)).

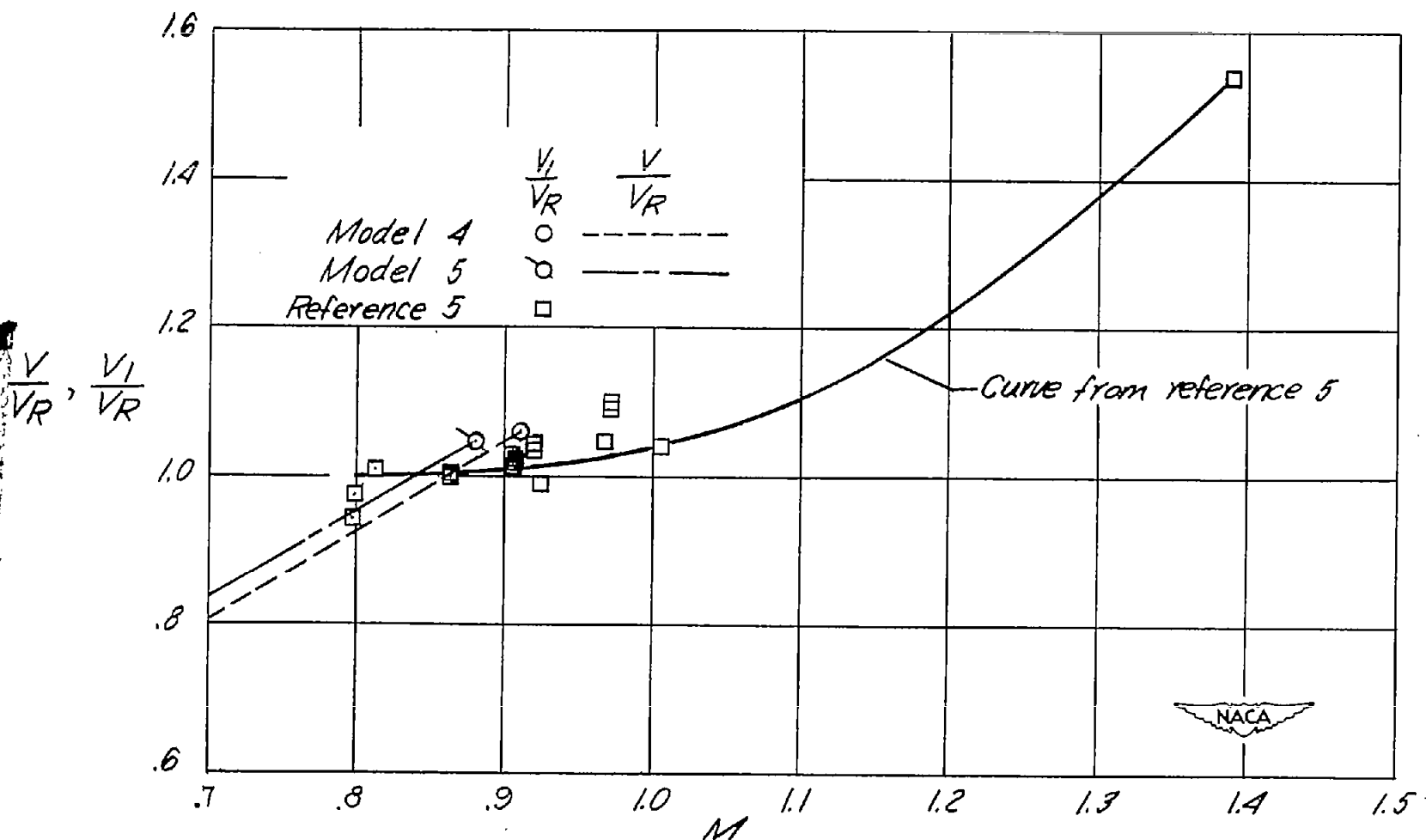
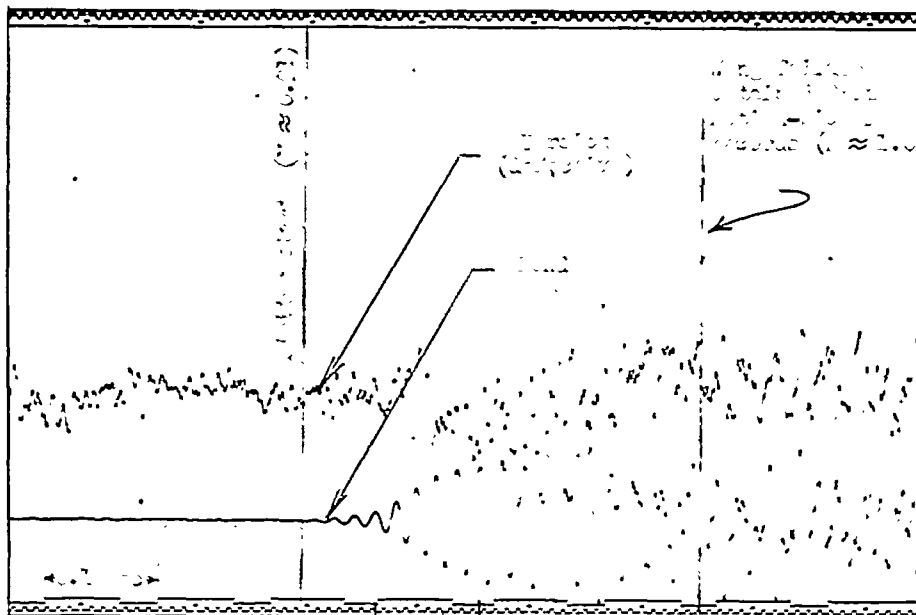
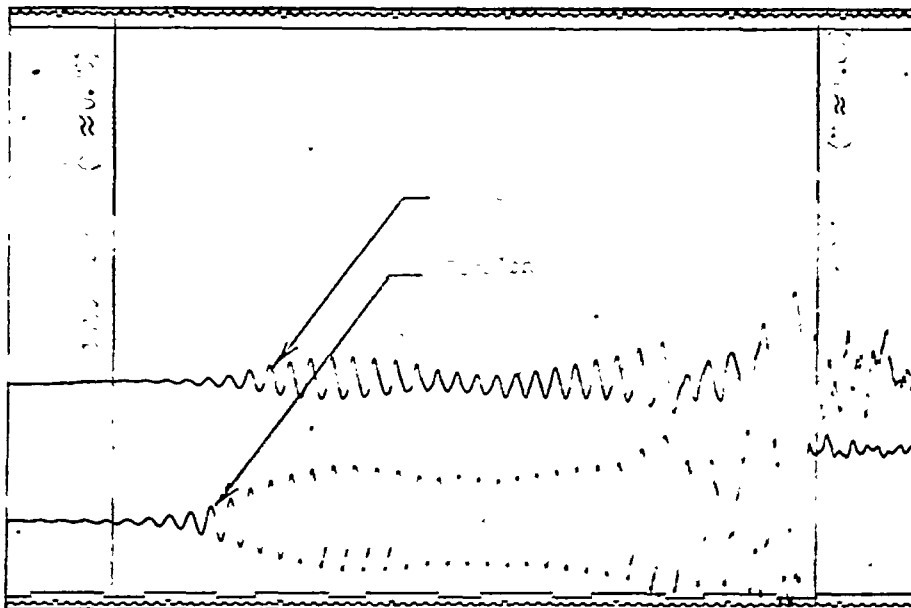


Figure 6.- Comparison of flight test results with data from reference 5.



(a) Model 4.



(b) Model 5.



Figure 7.- Portions of actual telemeter records showing time histories of bend and torsion strain-gage recordings.